Rev. Mexicana Astron. Astrof., 13, 107-113 (1986)

ELONGATED STRUCTURES NEAR STARS: JETS OR PROJECTION EFFECTS?

J. Cantó, A. Sarmiento, L.F. and L.F. Rodríguez

Instituto de Astronomía
Universidad Nacional Autónoma de México

Received 1986 May 26

RESUMEN

Observaciones recientes en las longitudes de onda correspondientes a las regiones de radio, infrarrojo y visible del espectro han mostrado la existencia de estructuras gaseosas, pequeñas y elongadas, que aparecen emanar de algunas estrellas. Estas estructuras son frecuentemente interpretadas como chorros cuya naturaleza es quizá similar a la de los chorros observados en objetos extragalácticos. En este trabajo proponemos que dichos "chorros" pueden simplemente deberse a la luz emitida por, o reflejada en las paredes de las cavidades que se forman alrededor de las estrellas cuando el viento de las mismas barre el medio gaseoso en sus alrededores. La radiación de las paredes de dichas cavidades, al ser observada desde ciertas posiciones, aparece como estructuras elongadas; un efecto de proyección que ilustramos mediante un modelo sencillo.

Discutimos también algunos casos bien conocidos de objetos, tanto jóvenes como evolucionados (PV Cep, R Mon, R CrA, G34.3 + 0.2, R Aqr, HH57, HL y XZ Tau y NGC 6302) donde este efecto de proyección puede estar operando.

ABSTRACT

Recent observations in radio, infrared and visible wavelengths have revealed the presence of small, elongated gaseous structures that appear to emanate from stars. These structures are frequently interpreted as jets, perhaps similar in nature to those observed in extragalactic objects. We argue that these apparent "jets" could simply be light emitted by or reflected from the walls of the cavities expected to be formed when the winds of these stars drive their surrounding gaseous medium away. When viewed from certain positions the radiation from the walls of these cavities appears to the observer as elongated structures. A simple model is presented to illustrate this projection effect.

We also discuss some well known sources both young and evolved (PV Cep, R Mon, R CrA, G34.3 + 0.2, R Aqr, HH57, HL and XZ Tau and NGC 6302), where this projection effect may be at work.

Key words: **STARS-CIRCUMSTELLAR SHELLS – STARS-WINDS**

I. INTRODUCTION

Gaseous outflows are now known to be a common phenomenon related to stars of recent formation (Rodríguez *et al.* 1982; Bally and Lada 1983; Edwards and Snell 1983; Calvet, Cantó and Rodríguez 1983; Cantó *et al.* 1984, Lada 1985). In a good number of sources the outflow geometry is bipolar, or at least anisotropic, pointing to the presence of a focusing agent. While some authors propose an originally isotropic stellar wind that is later focused by an external structure of circumstellar (Snell, Loren and Plambeck 1980; Rodríguez *et al.* 1986) or interstellar (Cantó *et al.* 1981) dimensions, others have suggested that the wind leaves the star anisotropically (Hartmann and MacGregor 1982; Mundt *et al.* 1984). With the continuous improvement of radio, infrared and optical imaging it has been possible to search for structures of small dimensions that could elucidate the real nature of the focusing mechanism.

Indeed, during the last few years several groups have reported the detection of elongated, faint structures in close association with young stars and Herbig-Haro (HH) objects. These structures have typical projected dimensions of $\sim 0.1 \times 0.001$ pc and are usually evident in deep Hα and [S II] images. Their line emission spectrum, similar to that of HH objects, may appear shifted by ~ 100 km s^{-1} with respect to the velocity of the star and occasionally may show velocity gradients. Examples of these elongated structures have been found associated with AS353A (Mundt, Stocke and Stockman 1983); HH12 (Strom, Strom and Stocke 1983), L1551 and HH101 (Morgan *et al.* 1984), DG Tau and XZ Tau (Mundt and Fried 1983), HH46-47 (Graham and Elias 1983), Haro 6-5B, HH33-40, HH19 and 1548C27 (Mundt *et al.* 1984), HH57 (Graham and Frogel 1984; Reipurth 1985) and HH34 (Reipurth *et al.* 1986). In these papers, the observed structures have been interpreted as jets collimated in the immediate vicinity of the star. To a lesser extent, elongated structures near evolved stars have occasionally been interpreted as jets. Perhaps the best known case is

R Aquarii (Sopka *et al.* 1982; Kafatos, Hollis and Michalitsianos 1983). We present here a different model that proposes the observed elongated structures to be not jets but the projection of the emitting walls of a cavity created by the stellar wind in the surrounding molecular cloud or envelope. Cantó (1980), Cantó and Rodríguez (1980) and Barral and Cantó (1981) have shown that isotropic winds from stars embedded in clouds with a density gradient create ovoid-shaped cavities. The walls of these cavities are the surfaces where the sum of the ram pressure of the wind plus the centrifugal pressure of the gas flow resulting from the refracting shock equals the gas pressure of the ambient cloud. Part of the kinetic energy of the wind is thermalized by these oblique shocks, and upon cooling will radiate presenting a spectrum similar to those of the HH objects. The glowing walls of these cavities, when projected on the observer's line of sight, may appear as elongated structures, Although we do not discuss in this paper the kinematical properties of these elongated structures, we should mention that we expect them to be similar to the observed ones. Indeed, since the shocked stellar wind retains an appreciable fraction of the original momentum and kinetic energy, the emitting flow along the walls of the cavity will have a velocity of the order of the velocity of the wind. Thus, under certain conditions we expect the elongated structures to show appreciable radial velocities with respect to the molecular background.

In §II we present a simple model to illustrate the projection effect. As mentioned in the abstract the model presented can explain the appearance of elongated structures due to either reflection, photoionization or shock excitation. In §III we discuss examples of several sources of relatively large angular dimensions where the presence of this effect is more evident, and compare them to some examples obtained with the model. We summarize our conclusions in §IV.

II. THE MODEL

In this section we present a simple model that roughly describes the expected spatial emission from the emitting walls of an ovoid cavity created by a strong wind. The functions $z = f_1(x, y)$ and $z = f_2(x, y)$ describe the inner and outer boundaries of the emitting shell of the cavity (Figure 1). The xy-plane is on the plane of the sky. For simplicity, we choose a system of reference such that both functions are symmetric around the x-axis and whose origin lies at the vertex of $f_2(x, y)$. Let (x_s, y_s, z_s) denote the position of the star and let $\vec{s}$ be the distance vector from it to any point under consideration.

Assume that the power emitted per unit volume depends on the square of the density (n) of the material in the shell. Pressure balance at any point in the cavity requires

$$\rho_w V_{wn}^2 \sim nkT \ ,$$

where ρ_w is the mass density of the wind and V_{wn} its velocity component normal to the cavity. Let θ be the angle between $\vec{s}$ and the normal to the cavity. Since $\rho_w \propto s^{-2}$, the power emitted per unit volume will be proportional to $(\cos\theta/s)^4$ for an isothermal shell. Then, the surface brightness for optically thin emission can be written as

$$I(x, y) = k\, \ell(x, y) \left(\frac{\cos\theta}{s} \right)^4 e^{-\tau(x,y)} \ , \qquad (1)$$

where k is a constant, $\ell(x, y)$ is the depth of the emitting region at the position (x, y) and $e^{-\tau(x,y)}$ represents the extinction due to the material around the cavity. We have also assumed a thin shell which means that the emitting power per unit volume is the same along the line of sight; the condition for the shell to be thin, in terms of $f_1(x, y)$ and $f_2(x, y)$, is

$$|f_2(x, y) - f_1(x, y)| \ll \begin{cases} |f_2(x, y)| \\ \text{or} \\ |f_1(x, y)| \end{cases} . \qquad (2)$$

Under this approximation the surface of the cavity can be obtained using either f_1 or f_2. Choosing f_2, the $\cos\theta$ factor is given by

$$\cos\theta = \hat{n} \cdot \hat{s} =$$

$$= \left\{ (x_s - x)(\partial f_2/\partial x) + (y_s - y)(\partial f_2/\partial y) + (f_2 - z_s) \right\} \times$$

$$\times [1 + (\partial f_2/\partial x)^2 + (\partial f_2/\partial y)^2]^{-1/2} \qquad (3)$$

$$\times [(x - x_s)^2 + (y - y_s)^2 + (f_2 - z_s)^2]^{-1/2} \ ;$$

where

$$\hat{n} = \frac{\partial\vec{r}/\partial x \times \partial\vec{r}/\partial y}{|\partial\vec{r}/\partial x \times \partial\vec{r}/\partial y|} =$$

$$= \frac{-(\partial f_2/\partial x)\,\hat{i} - (\partial f_2/\partial y)\,\hat{j} + \hat{k}}{[1 + (\partial f_1/\partial x)^2 + (\partial f_2/\partial y)^2]^{1/2}} \qquad (4)$$

and

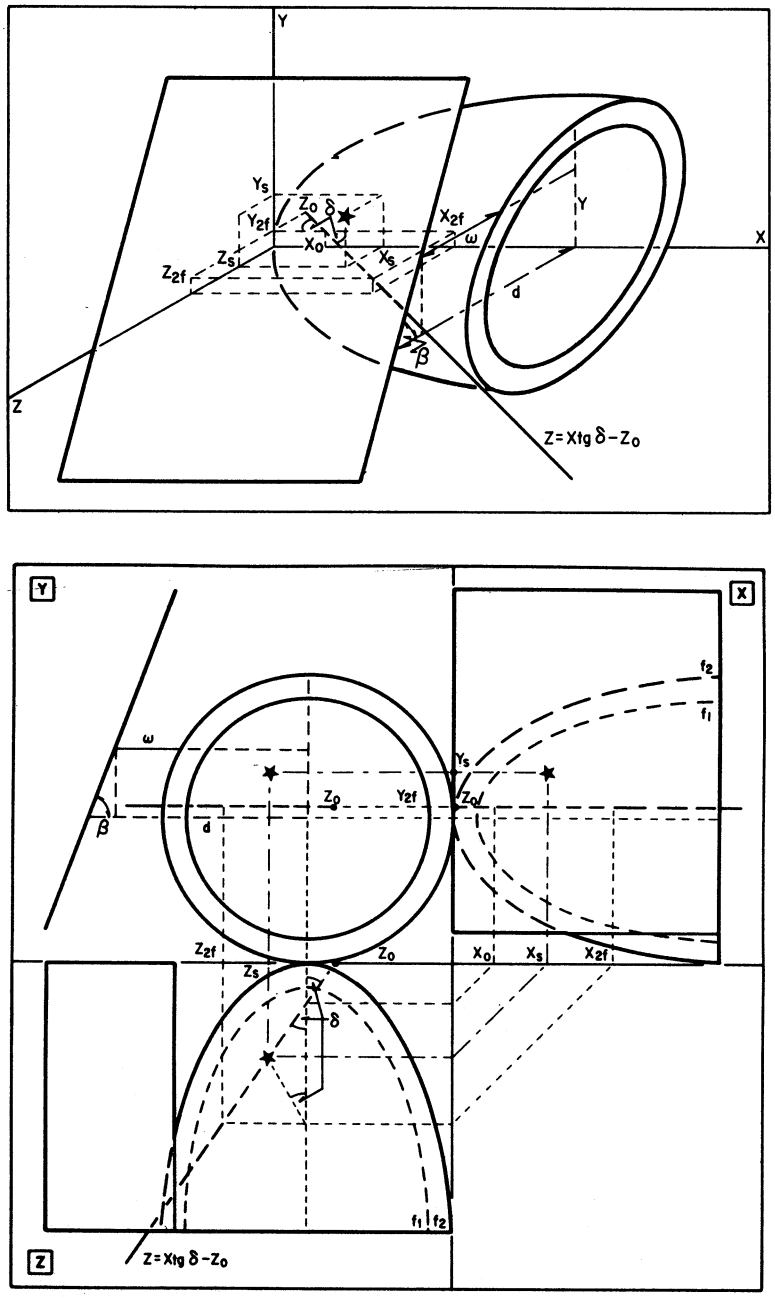

Fig. 1. Schematic representation of the cavity around the exciting star. f_1 and f_2 are the functions describing the boundaries of the emitting shell and the star is located at (x_s, y_s, z_s). The emitting cavity is immersed in a cloud whose exterior surface is a plane at a distance d from the axis of symmetry, and tilted by an angle β. The line of sight makes an angle δ with respect to the X-Y plane. The remaining parameters are defined in the text.

$$\hat{s} = \frac{\vec{r} - \vec{r}_s}{|\vec{r} - \vec{r}_s|} =$$

$$= \frac{(x - x_s)\,\hat{i} + (y - y_s)\,\hat{j} + (f_2 - z_s)\,k}{[(x - x_s)^2 + (y - y_s)^2 + (f_2 - z_s)^2]^{1/2}} \qquad (5)$$

have been used for the last equality in equation (3).

The value of $\ell(x, y)$ is given by the distance between the intersections of the line of sight with the functions $f_1(x, y)$ and $f_2(x, y)$. The line of sight may be represented by

$$y = y_\ell \qquad (6a)$$

$$z = (x - x_0)\,\mathrm{tg}\delta = x\mathrm{tg}\delta - z_0 \quad . \tag{6b}$$

where δ is the angle the line of sight makes clockwise with the xy-plane (Figure 1). The points $(x_0, y_\ell, 0)$ and $(0, y_\ell, z_0)$ indicate the intersections of the line of sight with the xy- and yz-planes, respectively.

If $|y_\ell| < |f_1(x, y)|$, the depth of the frontal emitting region ℓ is therefore given by

$$\ell_f(x,y) = [(x_{2f} - x_{1f})^2 + (z_{2f} - z_{1f})^2]^{1/2} =$$

$$= [(x_{2f} - x_{1f})^2 +$$

$$+ \left\{f_2(x_{2f}, y_\ell) - f_1(x_{1f}, y_\ell)\right\}^2]^{1/2} \tag{7a}$$

where the subscripts 1f and 2f indicate the coordinates of the intersections of eqn. (6) with the frontal halves of $f_1(x, y)$ and $f_2(x, y)$, respectively. The depth of the backless emitting region ℓ_b is obtained in a similar way and is denoted by coordinates with a 1b or a 2b subscript. The total depth of the emitting region is

$$\ell(x,y) = \ell_f(x,y) + \ell_b(x,y) .$$

If $|f_1(x, y)| \leq |y_\ell| \leq |f_2(x, y)|$ the depth of the emitting region is given by

$$\ell(x,y) = [(x_{2f} - x_{2b})^2 + (z_{2f} - z_{2b})^2]^{1/2} =$$

$$= [(x_{2f} - x_{2b})^2 +$$

$$+ \left\{f_2(x_{2f}, y_\ell) - f_2(x_{2b}, y_\ell)\right\}^2]^{1/2} \tag{7b}$$

As mentioned before, the extinction due to the material enveloping the shell-star system [whose density determines the shape of the shell, i.e., $f_1(x, y)$ and $f_2(x, y)$] is modelled through the multiplicative factor $e^{-\tau(x,y)}$ in eqn. (1). The opacity $\tau(x, y)$ is assumed to be proportional to the density of the enveloping material (n_c) times the width of the cloud (ω) (see Figure 1). Choosing for the cloud around the system a flat exterior surface described by $z = d - y\cot\beta$ (i.e., a plane whose distance from the xy-plane in the xz-plane is d and whose inclination with respect to the xz plane is β), the variable width of the cloud surrounding the shell is then given by the distance between the intersection of the line of sight with the flat exterior surface and the intersection of the line of sight with the frontal half of the shell, i.e.,

$$\omega(x,y) = [(x_p - x_{2f})^2 + (z_p - z_{2f})^2]^{1/2} =$$

$$= [(x_p - x_{2f})^2 +$$

$$+ (d - y_\ell \cot\beta - (x_{2f} - x_0)\mathrm{tg}\delta)^2]^{1/2} , \tag{8}$$

where the subscript p indicates the coordinates of the intersection of the line of sight with the flat exterior surface of the cloud, i.e.,

$$x_p = (d - y_\ell \cot\beta + z_0)/\mathrm{tg}\delta; \quad y_p = y_\ell ; \qquad z_p = d - y_\ell \cot\beta . \tag{9}$$

The opacity is therefore given by

$$\tau(x, y_\ell) \propto n_c(x, y_\ell)\,[(x_p - x_{2f})^2 + (z_p - z_{2f})^2]^{1/2} . \tag{10}$$

The constant of proportionality may be determined by assuming a value for the opacity when looking directly into the star, i.e., assuming a value for

$$\tau_s \equiv \tau(x_s, y_s) \propto n_c(x_s, y_s) \times$$

$$\times \{[x_p - x_s - (z_{2fs} - z_s)\,\mathrm{tg}\delta]^2 + (z_p - z_{2fs})^2\}^{1/2} , \tag{11}$$

where

$$z_{2fs} = f_2\,(x_s + (z_{2fs} - z_s)/\mathrm{tg}\,\delta, y_s) . \tag{12}$$

From equations (10) and (11) one gets

$$\frac{\tau(x, y_\ell)}{\tau_s} = \frac{n_c(x, y_\ell)}{n_c\,(x_s, y_s)} \times$$

$$\times [(x_p - x_{2f})^2 + (z_p - z_{2f})^2]^{1/2} \times \tag{13}$$

$$\times \{[x_p - x_s - (z_{2fs} - z_s)/\mathrm{tg}\,\delta]^2 + (z_p - z_{2fs})^2\}^{-1/2} ,$$

with x_p, z_p given by eqns. (9) and z_{2f} given by eqn. (12). Finally, assuming that the density $n_c(x\ y)$ is inversely

proportional to the quotient $(s/\cos\theta)^2$, eqn. (13) may be rewritten as

$$\tau(x, y_Q) = \tau_s \left[(z_{2fs} - z_s)/\sin\delta\right]^2 \frac{\cos^2\theta}{\cos^2\theta_s} \times$$

$$\times \left\{ \left[x_p - x_s - (z_{2fs} - z_s)/\mathrm{tg}\,\delta\right]^2 + (z_p - z_{2fs})^2 \right\}^{1/2} \times \tag{14}$$

$$\times \frac{\left[(x_p - x_{2f})^2 + (z_p - z_{2f})^2\right]^{1/2}}{(x_{2f} - x_s)^2 + (y - y_s)^2 + \left[f_2(x_{2f}, y_s) - z_s\right]^2} ,$$

where $\cos\theta$ is given by eqn. (3) and $\cos\theta_s$ is accordingly given by

$$\cos\theta_s = \frac{1}{\left[(1 + (\partial f_2/\partial x)^2 + (\partial f_2/\partial y)^2\right]^{1/2}} = \frac{1}{|\vec{n}|} ,$$

where the derivatives are evaluated in (x_s, y_s).

Figure 2 (Plate) shows some examples of the elongated structures obtained using the previous model. In all cases, the symmetry axis is perpendicular to the line of sight ($\delta = 90°$), and the star, located on this axis, is denoted by a point. For the upper panels the functions describing the shell are two concentric ellipsoids. The optical depths towards the star (τ_s) are 1 for the left frame and 0 for the right one. The width of the cloud (ω) is twice the length of the semiminor axis of the outer ellipsoid for the left frame and six times for the right one. The inclinations (β) are 30° and 90° respectively.

For the left lower frame a fourth order polynomial has been chosen in order to simulate the shape of a bipolar nebulae. The optical depth (τ_s) is 1, the width (ω) is five times the width of the waist and the inclination (β) is 90°. The right lower frame represents two concentric paraboloids. The values for the optical depth and the inclination are 2 and 30° respectively, and the width of the cloud is 8 times the distance from the star to the tip of the outer paraboloid.

Since some nebulae are expected to be excited by photoionization rather than by a shock, the example presented in the right upper frame has been calculated assuming that the density of material in the shell is proportional to r^{-1} and dropping the $\cos\theta$ factor.

In order to obtain images similar to those of photographic plates a saturation level has been set in all but the upper right panel. That is, all points with surface brightness greater than a certain threshold are equalled to this threshold. No saturation was imposed to the right upper panel since this case is intended to mimic radio observations. From the results presented above it is clear that one can easily reproduce many of the elongated structures observed so far.

In the following section a brief discussion on some well known sources is provided to further substantiate the idea of elongated structures being projection effects. We have selected sources of relatively large angular size where the pertinent structures are well resolved spatially.

III. OBSERVATIONAL EXAMPLES

In this section we show some examples taken from the literature where we believe that the elongated structures observed could be due to the projection effect previously discussed. See Figure 3 (Plate).

a) *PV Cephei*

The variable star PV Cep has an associated nebula, GM29 (Gyulbudaghian and Magakyan 1977), also time-variable (Cohen *et al.* 1981). Levreault (1984) detected an extended bipolar outflow associated with PV Cep. On the POSS red plate (see Figure 3*a*) GM24 appears as an elongated jet-like structure. In more recent epochs a cometary nebula has appeared with PV Cep at its tip (Cohen *et al.* 1981). The present shape of GM29 confirms the notion that the elongated structure seen in the POSS plate is the eastern edge of the cavity that is illuminated by PV Cep (see Figure 3*a*).

b) *R Monocerotis*

R Mon is associated with the cometary nebula NGC 2261 (Hubble's Variable Nebula). Cantó *et al.* (1981) showed that R Mon is associated with a low velocity bipolar outflow and that NGC 2261 is most probably one of the lobes of a bipolar nebula, the other being obscured by an interstellar toroid. In Figure 3*b* we can see that NGC 2261 has on its east side an elongated extension. Again, this feature is caused by light from R Mon reflected on the walls of the cavity, as indicated by the study of Jones and Herbig (1982).

c) *R Coronae Australis*

An elongated nebulosity associated with R CrA has been interpreted by Ward-Thompson *et al.* (1985) as a jet probably emanating from the star (see Figure 3*c*). This structure has P.A. $\cong$ 135°. However, the CO bipolar outflow found by Levreault (1985) has P.A. $\cong$ 90°. Ward-Thompson *et al.* (1985) have proposed that the optical "jet" is being collimated by a circumstellar disk with different orientation than the interstellar disk focusing the CO outflow. Alternatively, we propose that there is only one structure with its plane in the N-S direction. The optical "jet" is simply light emitted or reflected by the southern edge of the eastern cavity.

d) *G34.3 + 0.2*

This ultracompact radio H II region has a "cometary" shape, with the tail extending to the west (Reid and Ho 1985). The high dynamic range map of Garay, Rodríguez

and van Gorkom (1986) made at 2-cm with the *VLA* revealed a more complex shape (Figure 3*d*). In particular, we note the elongated structure running from the core region to the west. In this case we are observing free-free emission from the ionized northern wall of the cavity created by the wind of the exciting star or stars of G34.3 + 0.2. This suggestion is consistent with the interpretation of Garay *et al.* (1986), who propose that G34.3 + 0.2 is embedded in the western edge of a molecular slab and has evacuated ionized gas in the direction of lowest density.

e) *R Aquarii*

This symbiotic system is associated with an extended optical nebulosity of complex shape. The emission is dominated by two intersecting arcs extending about 2′ in the E-W direction (Figure 3*e*). With the *VLA* at 6-cm Sopka *et al.* (1982) detected continuum emission from the core of the region and from an extension at a P.A. of 24°. This structure has been interpreted by Sopka *et al.* (1982) and Kafatos, Hollis and Michalitsianos (1983) as a jet feature, probably ejected by the symbiotic system. On the other hand, Solf and Ulrich (1985) have proposed, based on their kinematical data that the structures of the R Aquarii nebula are not jets. We believe that the nebulosity associated with R Aquarii has a bipolar morphology and that the radio jet is simply one of the four "horns" that characterize the morphology of the central parts of this type of nebula (see Figure 3*e* and the models of Morris 1981). If our speculation is correct, very deep radio maps of R Aquarii should show *four* elongations producing an X-shaped source.

It is interesting to note that the "horns" in R Aquarii bend and intersect again far from the central objects. This focusing effect could be related to that proposed by Cantó and Rodríguez (1980) and Barral and Cantó (1981) for the formation of Herbig-Haro objects.

f) *NGC 6302*

This young planetary nebula exhibits a bipolar or "butterfly" shape in the optical, with the lobes extending in the E-W direction. The radio observations of Rodríguez *et al.* (1985) indicate that this morphology is influenced by the presence of a dense gaseous torus at the core whose axis of symmetry is similar to that of the optical lobes. The western lobe extends relatively far ($\sim 1'$) from the core region and transforms into two elongated arcs that intersect in a nebulous spot (Figure 3*f*, and plate 3 of Meaburn and Walsh 1980). We interpret these arcs as emission from the walls of the cavity created in the surrounding nebulosity by the wind of the central star of NGC 6302. As in the case of R Aquarii, the convergence of these arcs may be explained by the focusing mechanism of Cantó and Rodríguez (1980).

g) *HH57*

This is a low excitation Herbig-Haro object first reported by Schwartz (1977). Figure 3*g* shows a photograph taken with a narrow interference filter centered on Hα (but also trasmitting the adjacent [N II] lines) by Graham and Frogel (1985). The HH object and two well defined arcs extending N-S are clearly seen. The arcs connect the exciting source [an FU Ori-type star which just flared 3-4 yrs ago; Graham (1986), Graham and Frogel (1985)] with the HH-objects. These arcs most likely represent the projection, on the plane of the sky, of the emitting wall of the cavity created by a strong wind from the exciting source, as proposed by Cantó and Rodríguez (1980) in their focusing model.

h) *HL and XZ Tau*

These two young stars are located in the dark cloud L1551, the same containing the archetypal bipolar outflow. Calvet, Cantó and Rodríguez (1983) found a second outflow in this cloud that is probably associated with HL and XZ Tau. High-angular resolution mapping in CO of the flow is found in Torrelles *et al.* (1986). Mundt and Fried (1983) found two jet-like features, one directed northeastward and the other southward of the stellar pair. Figure 3*h* shows [S II] images, obtained at different radial velocities with a narrow-band filter tilting technique by Morgan *et al.* (1984). It is obvious from these images that the two jet-like features do not point directly at any of the stars, but inbetween them. Brown, Mundt and Drake (1985) recently found a radio continuum source about 3″ south of the tip of the northern feature. This source is interpreted as the most likely powering source of the jet-like structures (Mundt, Brugel and Bührke 1986). In our interpretation, however, the elongated structures seen in the optical together with the continuum source seen in the radio are the result of the interaction of the stellar wind of either HL or XZ Tau with the dense molecular environment. In Figure 4 we show the predicted appearance of an emitting cavity subject to different extinctions i.e., seen at different wavelengths. We can see that for wavelengths in which extinction is non-negligible (optical range) the observed structures are predicted to be elongated showing a jet-like appearance, while for wavelengths subject to negligible extinction (radio range) we expect to detect a rather compact source near the tip of the optical feature.

IV. CONCLUSIONS

We propose that in many cases the elongated structures observed near stars, both young and evolved, are not jets but a projection effect. This effect appears when the walls of the ovoid cavities produced by the wind of the associated star in the surrounding medium become luminous. The light emitted from these walls could be due to shock excitation, photoionization, or reflection. In the case of shock excitation, we expect the emitting material to show appreciable radial velocities. We present a model that accounts well for the morphologies observed in several well studied sources.

Our main conclusion is that elongated, slightly curved structures that appear to emanate from stars could well be a result of the projection effect discussed by us. However, our model can not explain the cases of very straight structures like the ones found in association with DG Tau B (Mundt and Fried 1983) and HH34 IRS (Reipurth *et al.* 1986).

We sincerely thank J.A. Graham and J.R. Walsh for the photographs of HH57 and R Mon, respectively, which are shown in Figure 3. We also thank CONACYT-Mexico for partial support (grant PCCBBNA-022688). This is Contribution No. 200 of the Instituto de Astronomía, UNAM, México.

REFERENCES

Bally, J. and Lada, C.J. 1983, *Ap. J.*, **265**, 824.
Barral, J.F. and Cantó, J. 1981, *Rev. Mexicana Astron. Astrof.*, **5**, 101.
Brown, A., Mundt, R. and Drake, S.A. 1985, in *Radio Stars*, eds. R.M. Hjellming and D.M. Gibson (Dordrecht: Reidel), p. 105.
Calvet, N., Cantó, J. and Rodríguez, L.F., 1983, *Ap. J.*, **268**, 739.
Cantó, J. 1980, *Astron. Astrophys.*, **86**, 327.
Cantó, J. and Rodríguez, L.F. 1980, *Ap. J.*, **239**, 982.
Cantó, J., Rodríguez, L.F., Barral, J.F. and Carral, P. 1981, *Ap. J.*, **244**, 102.
Cantó, J., Rodríguez, L.F., Calvet, B. and Levreault, R.M. 1984, *Ap. J.*, **282**, 631.
Cohen, M., Kuhi, L.V., Harlan, E.A., and Spinrad, H. 1981, *Ap. J.*, **245**, 920.
Edwards, S. and Snell, R.L. 1983, *Ap. J.*, **270**, 605.
Garay, G., Rodríguez, L.F. and van Gorkom, J.H. 1986, *Ap. J.*, **309**, 553.
Graham, J.A. 1983, *IAU Cir.* No. 3785.
Graham, J.A. and Elias, J.H. 1983, *Ap. J.*, **272**, 615.
Graham, J.A. and Frogel, J.A. 1985, *Ap. J.*, **289**, 331.
Gyulbudaghian, A.L. and Magakyan, T. Yu. 1977, *Pis'ma Astr. Zh.*, **3**, 113.
Hartmann, L. and MacGregor, K.B. 1982, *Ap. J.*, **257**, 264.
Jones, B.F. and Herbig, G.H. 1982, *Ap. J.*, **87**, 1223.
Kafatos, M., Hollis, J.M. and Michalitsianos, A.G. 1983, *Ap. J. (Letters)*, **267**, L103.
Lada, C.J. 1985, *Ann. Rev. Astron. Astrophys.*, **23**, 267.
Levreault, R.M. 1984, *Ap. J.*, **277**, 634.
Levreault, R.M. 1985, private communication.
Meaburn, J. and Walsh, J.R. 1980, *M.N.R.A.S.*, **193**, 631.
Morgan, J.S., Wolff, S.C., Strom, S.E. and Strom, K.M., 1984, *Ap. J. (Letters)*, **285**, L71.
Morris, M. 1981, *Ap. J.*, **249**, 572.
Mundt, R. and Fried, J.W. 1983, *Ap. J. (Letters)*, **274**, L83.
Mundt, R., Brugel, E.W. and Bührke, T. 1986, *Ap. J.*, submitted
Mundt, R., Stocke, J. and Stockman, H.S. 1983, *Ap. J. (Letters)*, **265**, L71.
Mundt, R., Bührke, T., Fried, J.W. Nëckel, T., Sarcander, M., and Stocke, J. 1984, *Astr. and Ap.*, **140**, 17.
Reid, M.J. and Ho, P.T.P. 1985, *Ap. J. (Letters)*, **288**, L17.
Reipurth, B. 1985, *Astr. and Ap.*, **143**, 435.
Reipurth, B., Bally, J., Graham, J.A., Lane, A. and Zealey, W.J. 1986, *Astr. and Ap.*, **164**, 51.
Rodríguez, L.F., Carral, P., Ho, P.T.P. and Moran, J. 1982, *Ap. J.*, **260**, 635.
Rodríguez, L.F., Cantó, J., Torrelles, J.M. and Ho, P.T.P. 1986, *Ap. J. (Letters)*, **301**, L25.
Rodríguez, L.F. *et al.* 1985, *M.N.R.A.S.*, **215**, 353.
Schwartz, R.D. 1977, *Ap. J. Suppl.*, **35**, 161.
Snell, R.L., Loren, R.B. and Plambeck, R.L. 1980, *Ap. J. (Letters)*, **239**, L17.
Solf, J. and Ulrich, H. 1985, *Astr. and Ap.*, **148**, 274.
Sopka, R.J., Herbig, G.H., Kafatos, M., and Michalitsianos, A.G. 1982, *Ap. J. (Letters)*, **258**, L35.
Strom, K.M., Strom, S.E. and Stocke, J. 1983, *Ap. J. (Letters)*, **271**, L23.
Torrelles, J.M., Anglada, G., Rodríguez, L.F., Cantó, J. and Barral, J.F. 1986, *Astr. and Ap.*, submitted.
Walsh, J.R. 1985, to appear in *IAU Symposium No. 115 Star Forming Regions*, eds. M. Peimbert and J. Jugaka (Dordrecht: D. Reidel).
Ward-Thompson, D., Warren-Smith, R.F., Scarrott, S.M. and Wolstencroft, R.D. 1985, *M.N.R.A.S.*, **215**, 537.

J. Cantó, L.F. Rodríguez and A. Sarmiento: Instituto de Astronomía, UNAM, Apartado Postal 70-264, 04510 México, D.F., México.

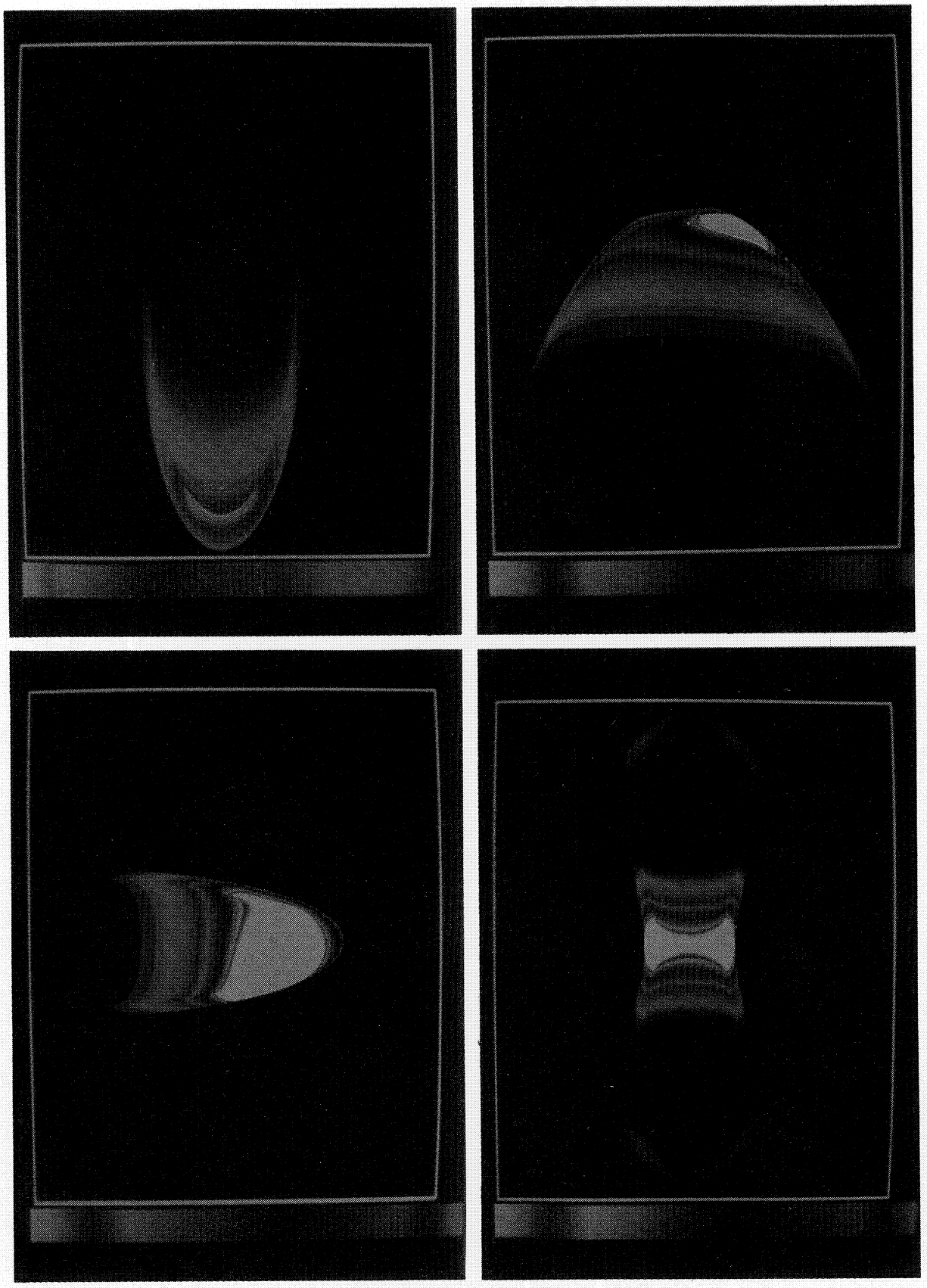

Fig. 2. Some examples of the elongated structures obtained with the model. The upper panels are concentric ellipsoids while the left lower frame is a fourth order polynomial and the right lower one are two concentric paraboloids. Note the similarities with the images of some of the objects shown in Figure 3 and discussed in the text.

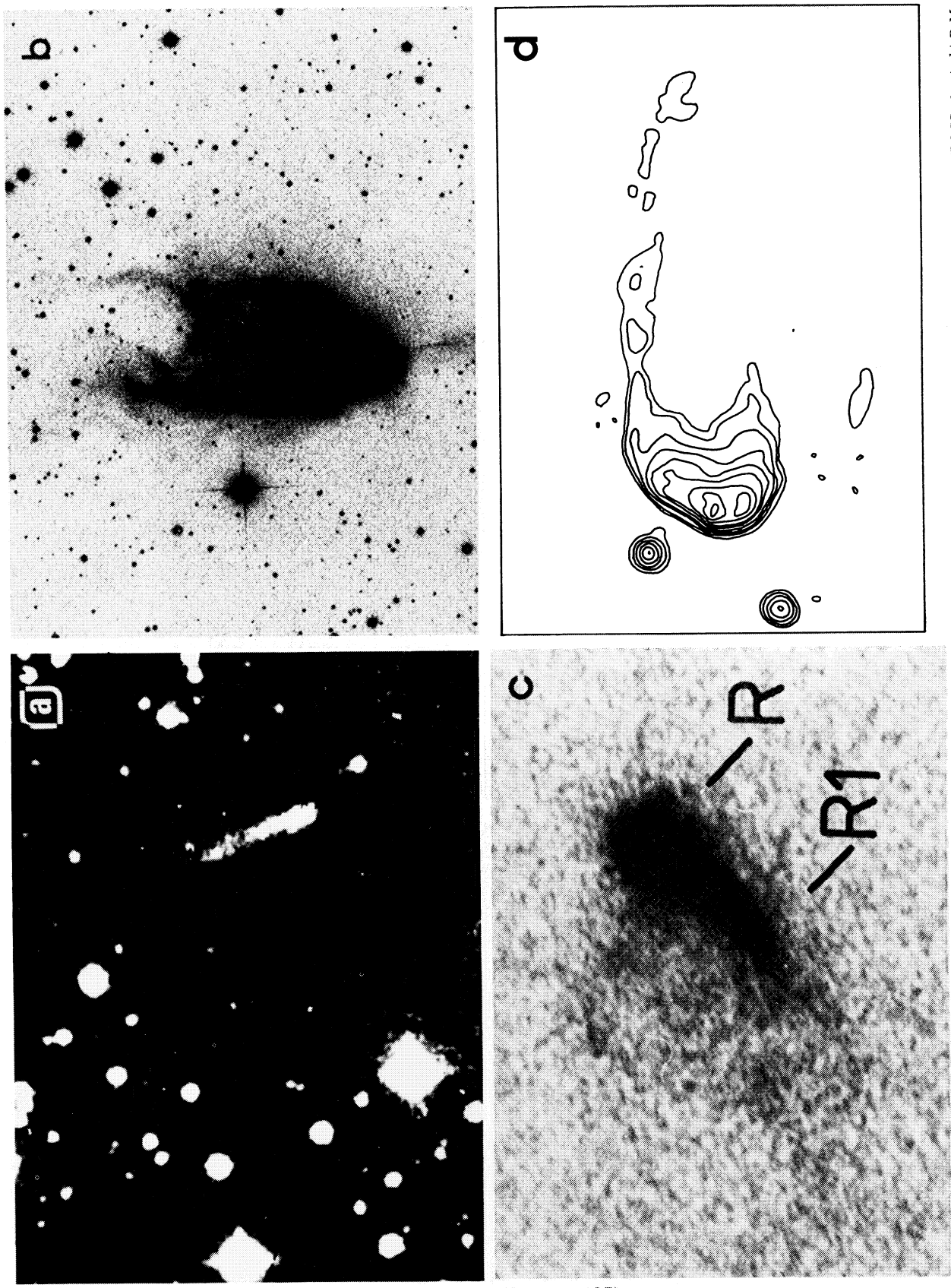

Fig. 3. Some examples where the observed elongated structures could be the projection, on the plane of the sky, of an emitting cavity. The are: *a)* PV Cep (POSS plate); *b)* R Mon (Walsh 1985); *c)* R CrA (Ward-Thompson *et al.* 1985); *d)* G34.3 + 0.2 (Garay, Rodríguez and Gorkom 1985).

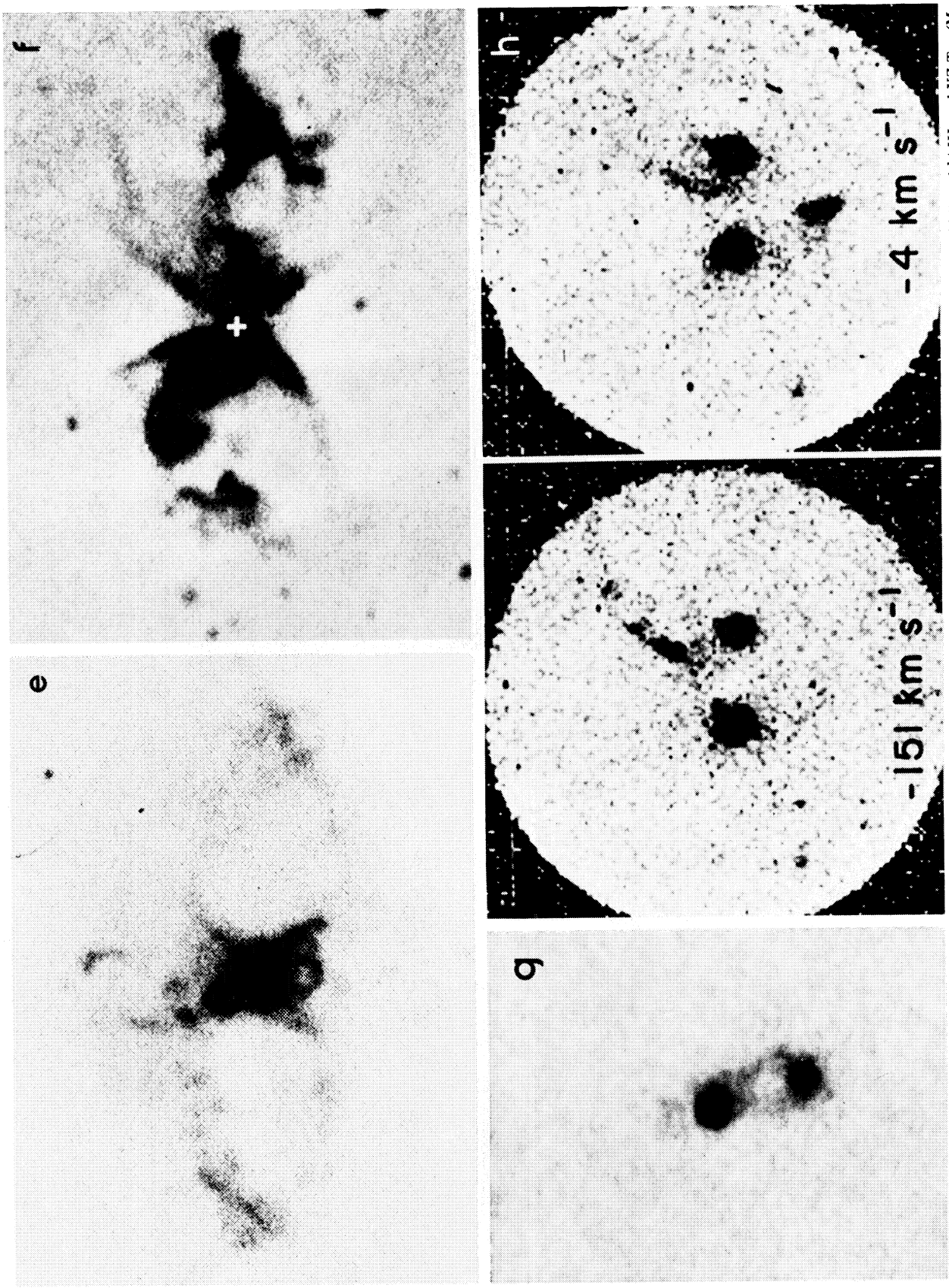

Fig. 3 (Continued) *e)* R Aqr. (Kafatos, Hollis and Michalitsianos 1983); *f)* NGC 6302 (Meaburn and Walsh 1980); *g)* HH57 (Graham and Frogel 1985) and *h)* HL and XZ Tau (Morgan *et al.* 1984), Note the morphological similarities with the structures obtained with the model (Figure 2).

J. Cantó *et al.* (See page 107)

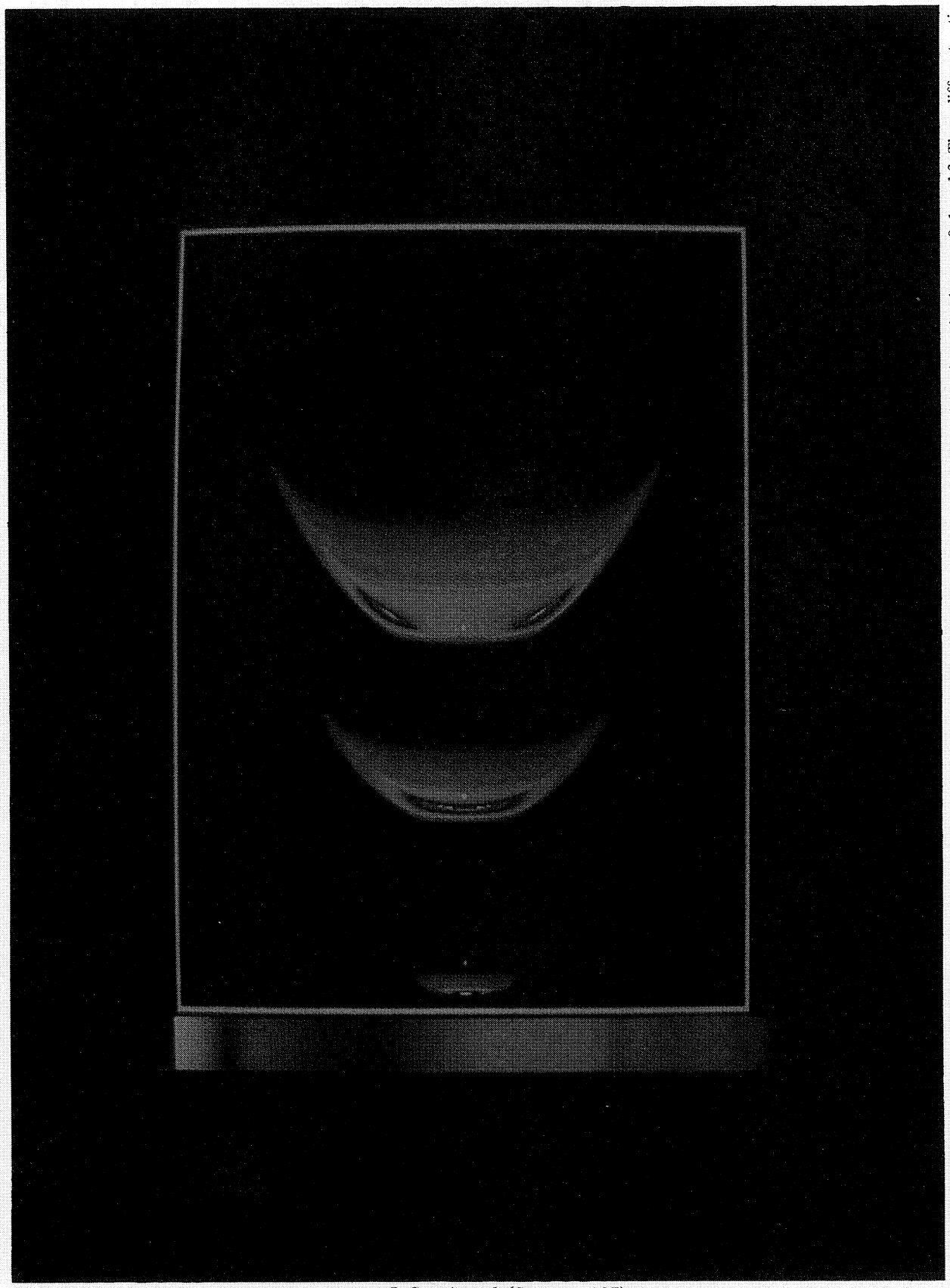

Fig. 4. Appearance of an emitting cavity subject to three different extinctions towards the star (see text). From left to right, the extinctions are 0, 1, and 3. These different extinctions simulate the expected radio (left), near-IR (center) and optical (right) appearance of the cavity. Note the changing appearance of the structure as extinction varies.

J. Cantó *et al.* (See page 107)